All-optical signal processing using nonlinear fibers

Kazuro Kikuchi, Kenji Taira, and Takuo Tanemura

Research Center for Advanced Science and Technology, University of Tokyo
4-6-1 Komaba, Meguro-Ku, Tokyo 153-8904, Japan
Phone: +81-3-5452-5123, Fax: +81-3-5452-5125
E-Mail: kikuchi@ginjo.rcast.u-tokyo.ac.jp

ABSTRACT

Third-order optical nonlinearity in optical fibers has attractive applications to all-optical signal processing that will be employed in future photonic networks. After reviewing the third-order nonlinear optical property of optical fibers, we describe some examples of all-optical signal processing devices, focussing on self-phase modulation (SPM), cross-phase modulation (XPM), and four-wave mixing (FWM).

Keywords: Optical Communications, Nonlinear Optics, Optical Signal Processing, Fiber Optics

1. INTRODUCTION

All-optical signal processing will play a major role in future photonic networks in order to fully utilize ultra-wide bandwidth of the optical carrier. The third-order optical nonlinearity is one of the most important effects for such all-optical signal processing.

Among various third-order nonlinear optical devices, a single-mode SiO_2 fiber is a promising candidate for a practical device. Low loss and well-controlled group-velocity dispersion (GVD) of the fiber make the interaction length very long. Moreover, a large power density is obtained inside the core. These properties greatly enhance the performance of nonlinear optical devices.

Recently, novel fiber designs have been demonstrated in order to improve nonlinear optical characteristics: The highly nonlinear dispersion-shifted fiber (HNL-DSF) having the nonlinear coefficient $\gamma \approx 20$ $km^{-1}W^{-1}$ is the most successful example [1]-[3]. Introduction of the holey fiber structure seems another interesting approach to increase the γ value through the extremely small core cross-section area [4]. Investigation on new highly-nonlinear glass materials other than SiO_2 has also been continued [5]-[7].

In this presentation, after reviewing the third-order optical nonlinearity of optical fibers, we describe our recent experimental results on all-optical signal processing, focusing on self-phase modulation (SPM) cross-phase modulation (XPM), and four-wave mixing (FWM) in optical fibers.

2. THIRD-ORDER OPTICAL NONLINEARITY IN OPTICAL FIBERS

When the light passes through a nonlinear optical material, the refractive index is slightly dependent on the electric field E as

$$\Delta n = n_2 |E|^2 \quad , \qquad (1)$$

where n_2 represents the nonlinear refractive index of the nonlinear material. In such a case, the phase ϕ of the light is changed by its power P as

$$\phi = \gamma PL. \qquad (2)$$

In Eq.(2), L denotes the propagation distance, and the third-order nonlinear coefficient γ, which mainly determines the performance of nonlinear optical devices, is given as

Active and Passive Optical Components for WDM Communications IV, edited by
Achyut K. Dutta, Abdul Ahad S. Awwal, Niloy K. Dutta, Yasutake Ohishi, Proc. of SPIE
Vol. 5595 (SPIE, Bellingham, WA, 2004) · 0277-786X/04/$15 · doi: 10.1117/12.580567

$$\gamma = n_2\omega_0/cA_{eff}, \qquad (3)$$

where ω_0 represents the frequency of the light, c the light velocity, and A_{eff} the effective core cross-section area. The parameter γ means the phase rotation angle per unit power and unit length, and is usually expressed in the unit of $km^{-1}W^{-1}$.

The γ value of a standard single-mode fiber (SMF) is 1.8 $km^{-1}W^{-1}$, whereas that of a dispersion-shifted fiber (DSF) is 2.6 $km^{-1}W^{-1}$. A_{eff} of DSF is smaller than that of SMF and Ge doped in the core enhances n_2. On the other hand, a highly nonlinear dispersion-shifted fiber (HNL-DSF) with the γ-value as high as 20 $km^{-1}W^{-1}$ has been developed. The γ value is greatly enhanced by the increased Ge concentration in the core and the reduced A_{eff}.

Recently, the holey-fiber structure with an extremely small A_{eff} has also been demonstrated. The γ-value of a SiO_2-based holey fiber reaches 70 $km^{-1}W^{-1}$.

Another approach to the enhancement of the fiber nonlinearity is to use a material having a nonlinear refractive index higher than that of the SiO_2 glass. Table I summarizes γ of the fibers drawn from various glass materials. It should be noted that increase in n_2 is usually accompanied by larger material GVD, which reduces the interaction length of devices. The reduction of propagation loss is also a crucial consideration in order to improve the device performance.

Table I Nonlinear fiber characteristics.

Material	SiO_2-GeO_2			SF57	As_2S_3	Bi_2O_3
Organization	Furukawa	Sumitomo	Southampton Univ.	Southampton Univ.	NTT	Asahi Glass U. of Tokyo
γ[$W^{-1}km^{-1}$]	25.1	10.4	70	640	~1000	1360
Loss [dB/km]	1.16	0.47	190	9000	600	1900
D @ 1.55 μm [ps/nm/km]	-0.08	0.42	-30	88	-400	-270
$(\partial D/\partial\lambda)$ [ps/nm^2/km]	0.013	0.0002	-0.6	N.A.	N.A.	~ 0.4
Remarks	[2]	Dispersion flattened [3]	Pure silica Holey fiber [4]	Holey fiber [5]	Step index [6]	Step index [8]

3. SPM-BASED SIGNAL PROCESSING

When a light passes through a fiber, the phase ϕ is changed by its own power P according to Eq.(2). This effect is called self-phase modulation (SPM). Therefore, when a short optical pulse with a high peak power is incident on a fiber, the spectrum is widely broadened through SPM. The broadened spectrum is often referred to as the super-continuum (SC). By manipulating such SC spectrum in the frequency domain, we can achieve various kinds of optical signal processing.

We previously proposed the use of a dispersion-flattened fiber (DFF) with a small normal GVD for flat and wideband SC generation [8]. Fig.1 shows the principle of flat spectral broadening. At short propagation distances, the spectrum broadens by SPM. The chirp induced by SPM is shown by the broken curve, which is given as the time-derivative of the pulse waveform. Since the chirp is folded, the spectrum has a deep ripple. When the GVD of the fiber is normal, the high frequency component travels through the fiber with a slower velocity, and the low frequency component does with a faster velocity. Therefore, the inflection points on the pulse waveform are pulled outside, and the pulse waveform is evolved into the bell shape. The chirp induced by this bell shape is linear between the inflection points, and the folded parts of the chirp move to edges of the pulse. Therefore, the energy included in the folded parts becomes smaller, resulting in the reduction of the ripple. The SC spectrum is relatively immune to the power, waveform and chirp of the input pulse. In addition, the high signal-to-noise ratio can be maintained during the SC generation process. It should be also noted that when an optical bandpass filter slices the SC spectrum, pulse widths are almost the same over the whole spectrum. Fig.2 shows a typical example of the SC spectrum, which is obtained by launching a 2-ps, 10-GHz pulse train on a 1-km-long HNL-DSF with β_2 = 2.2 ps^2/km.

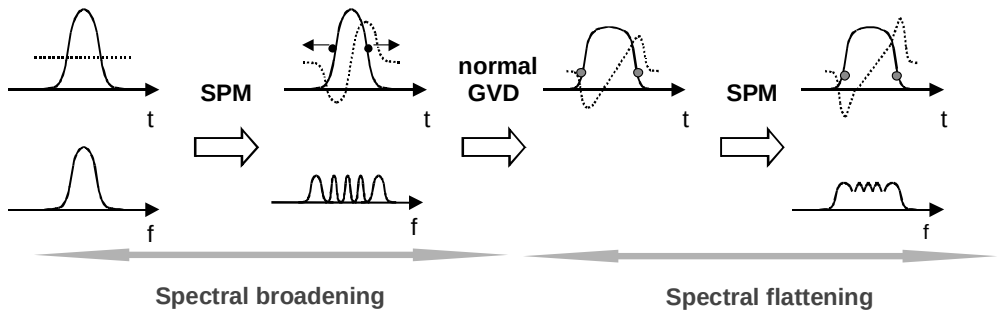

Fig.1 Principle of flat spectral broadening through the interaction between SPM and normal GVD.

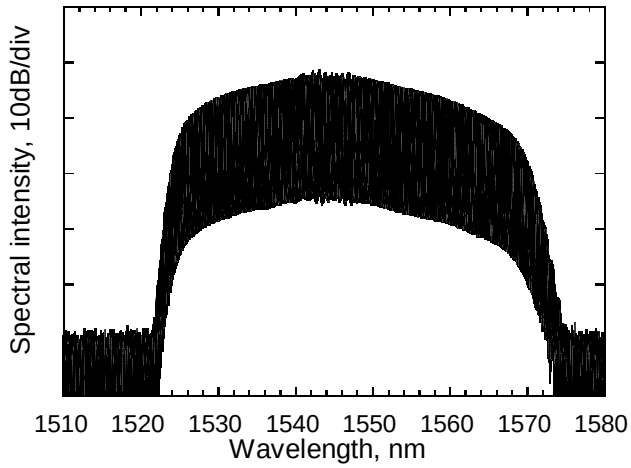

Fig.2 An example of a flat and wideband SC spectrum.

Broadening the spectrum of the input signal flatly and slicing the broadened spectrum, we can realize various kinds of all-optical signal processing circuit such as the wavelength converter and the all-optical 2R circuit. The above-mentioned characteristics of the SC generated from the normal GVD fiber are very attractive for these applications. The most straightforward application is the wavelength converter shown in Fig.3. An AWG slices the SC spectrum and optical switches select one of the wavelength channels. The second AWG leads the selected wavelength channel to the output port. This configuration can also be applied to wavelength broadcast/multicast.

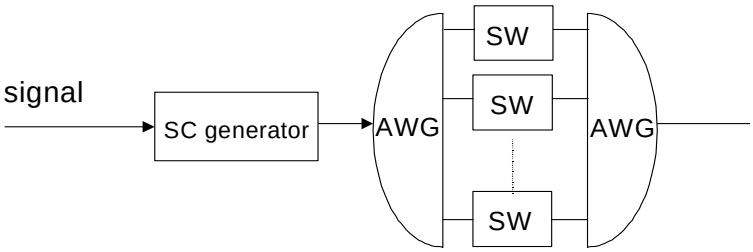

Fig.3 Construction of the wavelength converter.

Fig.4 shows the principle of the pulse reshaper based on the spectral filtering of the SC. When the input pulse with a pedestal is incident on the SC fiber, the pedestal component remains at the center wavelength, whereas the main pulse component shifts from the center wavelength in the SC spectrum. Therefore, as far as we slice the SC spectrum at off-center wavelengths, we can obtain pedestal-free pulses. This pulse reshaping function can realize the all-optical 2R circuit [9][10].

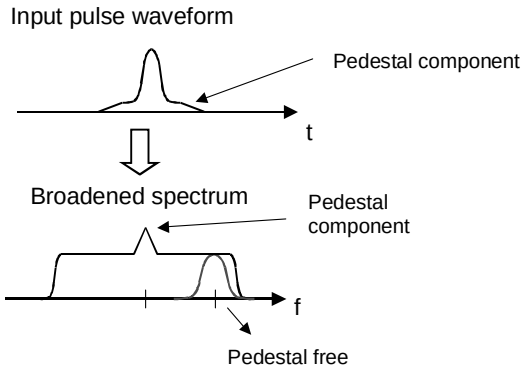

Fig.4 Principle of pulse reshaping by slicing of the SC spectrum

4. XPM-BASED SIGNAL PROCESSING

When a light passes through a fiber together with a pulse, its phase ϕ is changed by the power P of the pulse. This effect is called cross-phase modulation (XPM).

The nolinear optical loop mirror (NOLM) is a typical example of all-optical signal processing devices based on XPM. We consider a conventional NOLM switch shown in Fig.5. A signal light incident on the NOLM from the 3-dB coupler travels through the loop in both directions, whereas the control pulses launched on the NOLM from the WDM coupler travel through the loop in one direction.

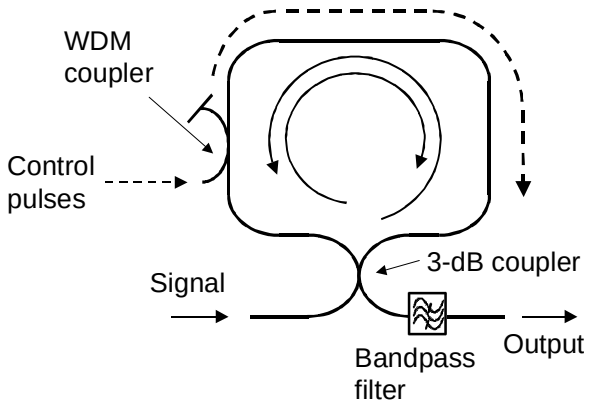

Fig.5 Basic structure of NOLM.

Since the response speed of the third-order nonlinear coefficient of SiO_2 is in the femtosecond region, the switching speed of the NOLM is potentially very fast. However, ultrafast operation of the NOLM has only been demonstrated in demultiplexing of OTDM signals, where the duty ratio of the base-clock pulse switching the data pulses is very low; on the other hand, in wavelength converters and optical 2R/3R switches, where the data pulses switch a CW light or a clock pulse train, it becomes difficult to maintain an adequate extinction ratio of the switch.

Fig.6 shows why a NOLM can never achieve the full-swing switching with the maximum extinction ratio. When control pulses are injected into the NOLM (Fig.6(b)), they induce the phase shift on the co-propagating signal light through XPM as shown in Fig.6(a). The phase shift is the replica of the waveform of the control pulses. On the other hand, the signal light counter-propagating with the control pulses suffers from XPM induced by the time-average power of the control pulses, and a constant phase shift appears on the signal light as shown in Fig.6(c). This is because the signal crosses many control pulses during propagation through the NOLM. These two signal lights interfere with each other at the output port of the NOLM, giving the output waveform shown in Fig.6(d).

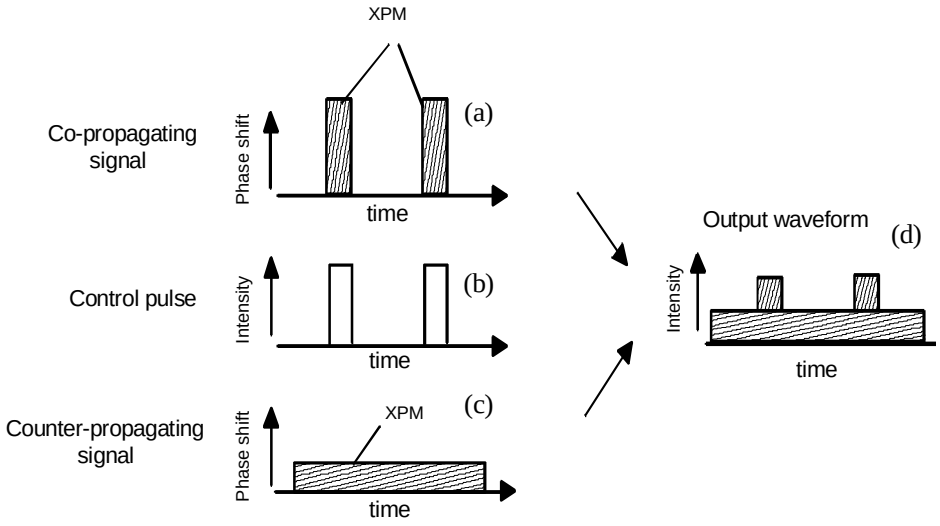

Fig.6 Mechanism of degradation of the extinction ratio.

Thus, we find that due to a constant phase shift on the signal light, the NOLM switch is not completely switched off in the space state, which limits the extinction ratio of the switch. Only in the case of the time-division demultiplexer, the extinction ratio is almost maximized, because the duty ratio of the control pulses is usually quite low. However, in wavelength converters and optical 2R/3R switches, where random data pulses acting as the control pulses switch a CW light or a clock pulse train, the extinction ratio is degraded significantly because of the high average power of the control pulses.

In order to cope with this difficulty inherent in the NOLM switch, we need to give a proper amount of optical bias between signal lights propagating through the same loop in opposite directions. We have recently developed a novel optical bias controller for a NOLM [11]. The part surrounded by broken lines in Fig.7 shows the optical bias controller placed inside the PM fiber loop. It consists of two Faraday rotators, cross-spliced PM fibers, and a fiber squeezer. Between the two Faraday rotators, polarization states of signal lights co-propagating and counter-propagating with the control pulse are orthogonal. Therefore, when we squeeze the fiber in the optical bias controller, signal lights traveling through the loop in both directions experience phase shifts different from each other. The optical bias thus generated can compensate for the phase shift of the signal light that is induced through XPM from the counter-propagating control pulses.

Eye patterns of the 10-Gbit/s signal wavelength-converted by the NOLM switch are shown in Fig.8. The left figure is obtained when the optical bias given by the controller is zero, that is, the conventional switching condition of the NOLM. The eye pattern is almost closed in this case. On the other hand, as shown in the right figure, well eye opening is obtained when the optical bias is optimized. This type of NOLM is potentially applicable to wavelength converters as well as 2R/3R circuits operating at 160 Gbps.

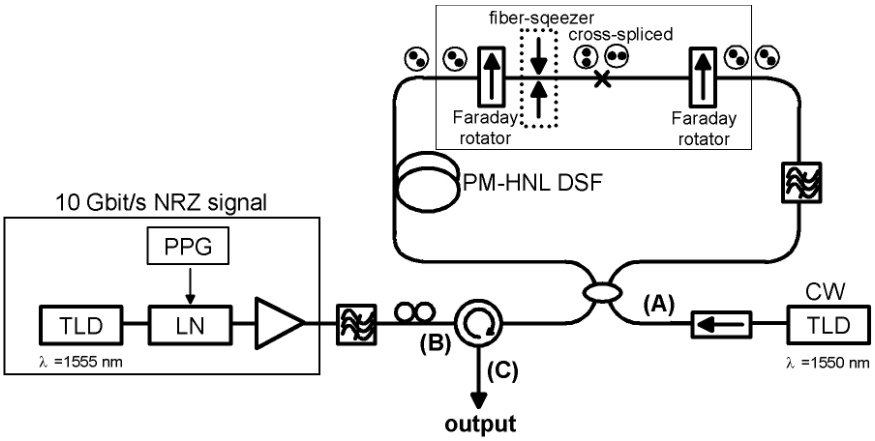

Fig.7 Experimental setup for wavelength conversion using a NOLM with an optical bias controller.

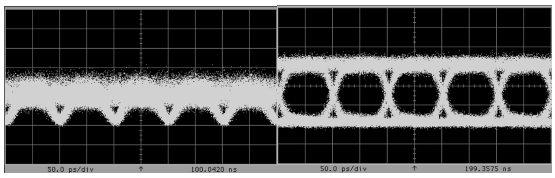

Fig.8 Eye patterns of the output signal [20 ps/div]
left: no bias, right: optimal bias.

The Kerr shutter is another all-optical signal-processing device using XPM. We have proposed a simple scheme for all-optical time-division add-drop multiplexer (ADM) based on the optical Kerr shutter [12].

The principle of the proposed ADM is shown in Fig. 9. Input OTDM signal 1 and 2 have linear polarizations that are orthogonal to each other. We prepare base-clock pulses with high peak powers, which are polarized 45° with respect to the input OTDM signals. When the signals and the base clock are incident on a Kerr medium, the Kerr rotation induces exchange of the polarization states of the two OTDM signals in the time slot, where the base-clock pulse exists. By using a polarization beam splitter (PBS) following the Kerr medium, respective OTDM signals are separated with one of their tributary channels exchanged.

By using a fiber-based Kerr shutter, one of 10-Gbit/s tributary channels is dropped from a 40-Gbit/s OTDM signal and a new tributary channel of another 40-Gbit/s signal is added simultaneously; we can thus achieve exchange of 10-Gbit/s tributary channels between two 40-Gbit/s OTDM signals.

Fig. 10 shows eye diagrams of output 1. Without the base clock, signal 1 is transmitted (Fig. 10 (a)), whereas signal 2 is attenuated (Fig. 10 (b)). When the base clock is present, the second tributary channel of signal 1 is extracted (Fig. 10 (c)), while that of signal 2 is inserted (Fig. 10 (d)). Owing to this ADM function, the second tributary channels of signal 1 and 2 are simultaneously exchanged. (Fig. 10 (e)). Thanks to the ultra-fast response time of the Kerr effect of optical fibers, the proposed scheme is applicable to 160 Gbit/s and higher.

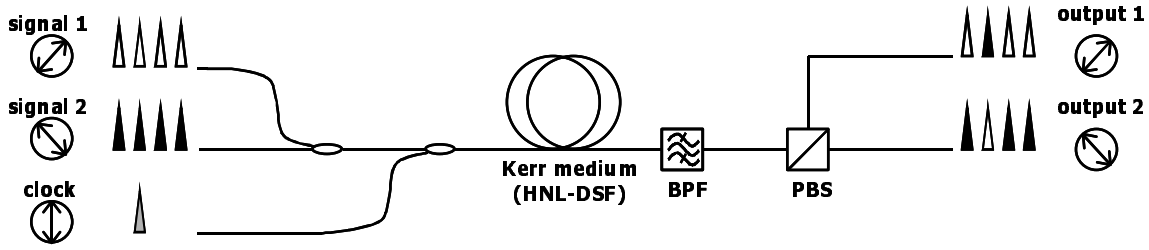

Fig. 9 Principle of the proposed all-optical time-division ADM.

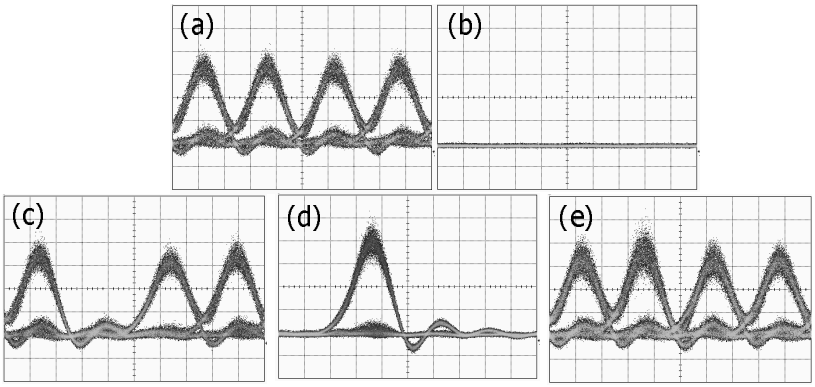

Fig. 10. Eye diagrams of output 1 in the presence of following inputs (10 ps/div): (a) signal 1. (b) signal 2. (c) signal 1 and clock. (d) signal 2 and clock. (e) signal 1, 2, and clock.

5. FWM-BASED SIGNAL PROCESSING

By the third-order nonlinearity, the wave mixing process occurs among three different frequency components ω_1, ω_2, and ω_3, and a new wave is created at $\omega_4=\omega_1+\omega_2-\omega_3$. This process called four-wave mixing (FWM).

When electric fields E_1 and E_2 at ω_1 and ω_2, respectively, are CW and E_3 at ω_3 carries information, the signal at ω_3 is converted to ω_4. Such an all-optical wavelength converter based on FWM in optical fibers has many attractive features such as high efficiency and low noise characteristics. As a special case, suppose that the frequency ω_1 of pump 1 is set in the normal GVD region, whereas the frequency ω_2 of pump 2 in the anomalous GVD region as shown Fig.11. The FWM effect in such a case can be understood in terms of the combination of SPM/XPM and GVD. When absolute values of GVD at these frequencies are almost the same, only sidebands A_{2+} and A_{1-}, which exist in between the two pump frequencies, experience the modulation instability (MI) gain. This MI gain enables us to realize highly efficient broadband wavelength conversion.

The mechanism generating such MI gain is explained in Fig.12 [13]. Phasors representing the pump and the single sideband move along circles, as illustrated by bold lines in Fig.12(a). Note that two phasors rotate in opposite

directions (a⇒ b⇒ c ⇒ d), and the phasor positions at time a, b, c, and d are shifted by π/2 radian between two pumps. First, XPM on pump 1 from pump 2 is considered. The phasor of pump 1 is stretched upward at time c and downward at a, corresponding to the amplitude of pump 2 at each time. Similar forces are experienced by pump 2. These effects are indicated by gray arrows in Fig. 12(a). Next, trajectories rotate around respective carriers due to GVD. Phasors of pump 1 and pump 2 rotate counterclockwise and clockwise, respectively. Rotation rates of two phasors are nearly equal, so that the two trajectories rotate symmetrically as illustrated in Fig.12(b). After rotation, phasors experience XPM again, and the trajectories transform as shown in Fig.12(c). By experiencing the GVD and XPM effects alternately in this way, the trajectories continue growing larger without deforming the circular shapes.

The MI gain thus generated is very flat over the band ranging from ω_2 to ω_1. Therefore, launching a signal at ω_1-Ω on the fiber, we can convert the signal into the idler at ω_2+Ω with high conversion efficiency. Furthermore, when two orthogonally polarized pumps are employed, the conversion efficiency becomes insensitive to the state-of-polarization (SOP) of the input signal light, which is strongly demanded in practical applications. By using the two-orthogonal-pump FWM scheme, we demonstrated a broadband wavelength converter with efficiency independent of the signal SOP. Fig.13 shows our experimental result. The conversion efficiency >0dB is achieved over 30 nm with polarization sensitivity less than 2 dB [14].

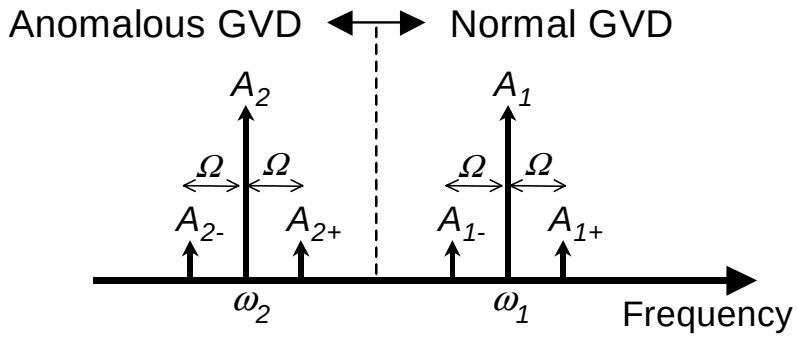

Fig.11 Frequency allocation in two-pump FWM.

When E_1 and E_2 are identical, the wave mixing process is called degenerate FWM. This configuration is effective for optical gate switching: $E_1(=E_2)$ is the clock pulse, which gates the signal E_3. Using degenerate FWM, we have demonstrated an all-optical time-division demultiplexer that enables us to demultiplex a 160-Gbit/s signal into 10-Gbit/s tributary channels with polarization sensitivity less than 0.5 dB [15].

Fig.14 shows the basic construction of the proposed polarization-diversity demultiplexer. The clock pulse and the signal pulse are incident on a short polarization-maintaining (PM) fiber before introduced into a four-wave mixer composed of a non-PM dispersion shifted fiber (DSF). The signal pulse has a random polarization state, whereas the clock pulse is linearly polarized 45 degrees with respect to the principle axis of the PM fiber.

As the PM fiber induces a group delay between the two linear polarization modes, an incident pulse is split into two pulses in time domain. The first and second pulses are linearly polarized along the fast and slow axes of the PM fiber, respectively, at the output of the PM fiber. The length of the PM fiber is adjusted so that the fast-axis and slow-axis components are not overlapped with each other. Two pulses split from the clock pulse have the same power; therefore, the clock pulse independently switches each polarization component of the signal pulse in the fiber four-wave mixer following the PM fiber. The bandwidth of the receiver placed at the fiber output is determined from the bit rate of tributary channels. Therefore, detected waveforms of the twin switched pulses are broadened and overlapped in the electrical domain due to the limitation of the receiver bandwidth. In such a case, the peak value of the overlapped waveform becomes independent of the polarization state of the input signal, and the polarization-independent time-division demultiplexing can be achieved.

Fig.15 shows the FWM spectrum, where “Signal" represent the spectrum of the 160-Gbit/s signal, “Pump" that of the 10-GHz clock pulse, and “Idler" that of the 10-Gbit/s demultiplexed signal. Figure 16 shows an example of the eye pattern of the demultiplexed signal, which is obtained by filtering the “Idler" wave in Fig.15. Well eye opening is maintained in arbitral polarization states of the incoming signal.

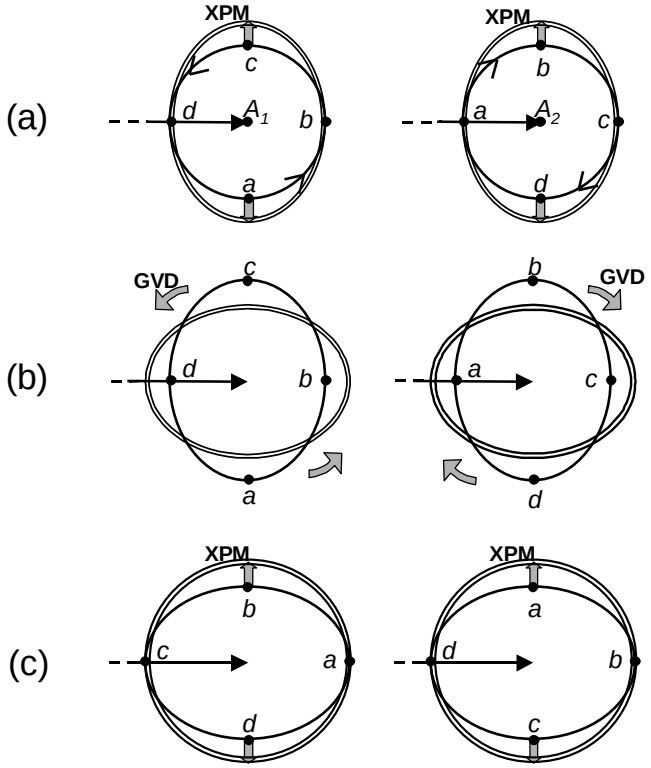

Fig.12 Evolution of phasors of two pumps under the influence of XPM and GVD.

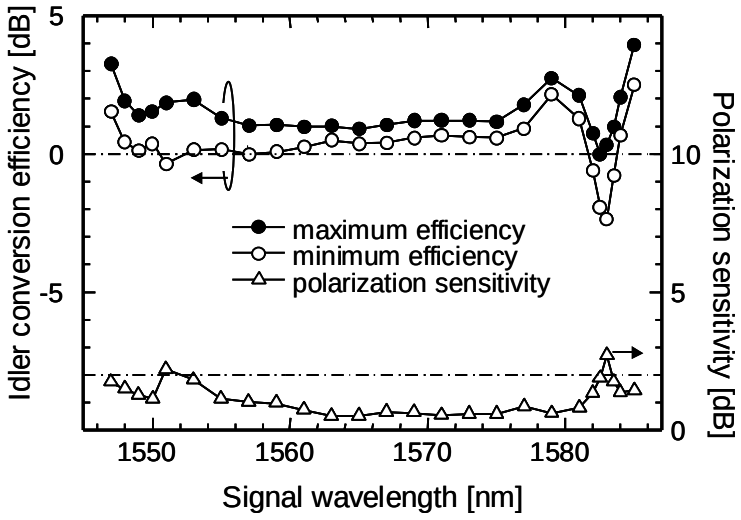

Fig.13 Wavelength conversion efficiency and polarization sensitivity in the two-pump FWM scheme.

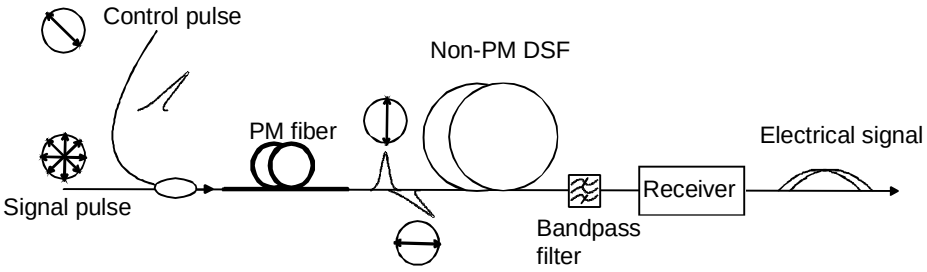

Fig.14 Principle of the polarization diversity scheme for an optical gate.

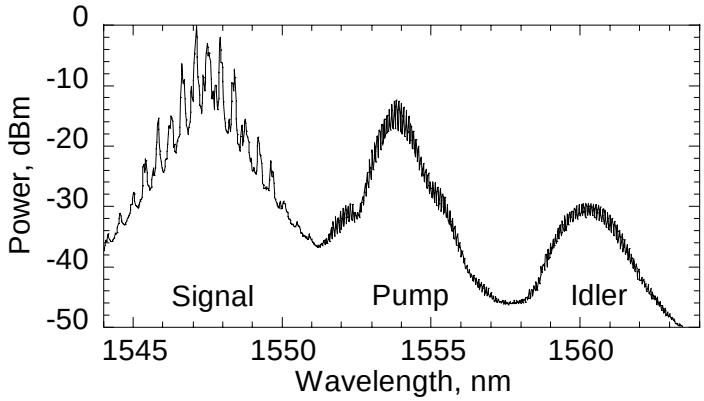

Fig.15 Spectra of the 160-Gbit/s signal, the 10-GHz clock pulse, and the 10-Gbit/s demultiplexed signal.

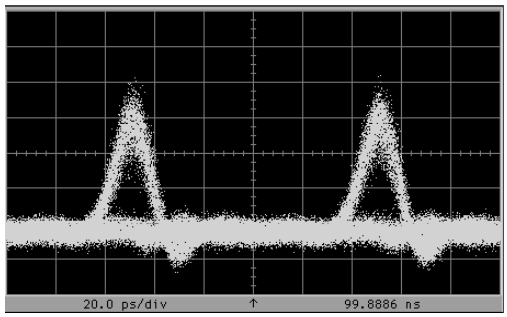

Fig.16 An example of the eye pattern of the demultiplexed signal [20 ps/div].

6. CONCLUSIONS

High optical nonlinearity and well-controlled GVD of SiO_2-based optical fibers can afford us a variety of optical signal processing functions. We have described some examples of such functions based on SPM, XPM and FWM.

Novel glass materials such as Bi_2O_3 and novel fiber structures such as the holey fiber are key technologies for future nonlinear devices; however, dispersion control and loss reduction are crucial considerations for practical applications of such nonlinear fiber devices.

REFERENCES

1. M.Onishi, T.Okuno, T.Kashiwada, S.Ishikawa, N.Akasaka, and M.Nishimura, "Highly nonlinear dispersion shifted fiber and its application to broadband wavelength converter," Integrated Optics and Optical Fibre Communications (IOOC'97) and European Conference on Optical Communications (ECOC'97), Edinburgh, U.K., Sept.22-25, 1997, paper TU2C.
2. J. Hiroishi, N. Kumano, K. Mukasa, R. Sugizaki, R. Miyabe, S. Matsushita, H. Tobioka, S. Namiki, and T. Yagi, "Dispersion slope controlled HNL-DSF with high γ of 25 W^{-1} km^{-1} and band conversion experiment using this fiber," European Conference on Optical Communications (ECOC'02), Copenhagen, Denmark, Sept.8-12, 2002, PD 1.5.
3. T. Okuno, M. Hirano, T. Kato, M. Shigematsu, and M. Onishi: "Highly nonlinear and perfectly dispersion-flattened fibres for efficient optical signal processing applications," Electron. Lett., vol.39, no.13, pp. 972-973, 2003.
4. P.Petropoulos, T.M.Monro, W.Belardi, K.Furuswa, J.H.Lee, and D.J.Richardson, "2R-regenerative all-optical switch based on a highly nonlinear holey fiber," Opt. Lett., vol.26, no.16, pp.1233-1235, 2001
5. T.M.Monro, K.M.Kiang, J.H. Lee, K. Frampton, Z. Yusoff, R.Moore, J.Tucknott, D.W.Hewak, H.N.Rutt, and D.J.Richardson, High nonlinearity extruded single-mode holey optical fibers," Optical Fiber Communication Conference (OFC'02), 17-22 March 2002, Anaheim, CA, USA., FA1.
6. M.Asobe, T.Kanamori, and K.Kubodera, "Ultrafast all-optical switching using highly nonlinear chalcogenide glass fiber," IEEE Photonics Technol. Lett., vol.4, no.4, pp.362-365, 1992
7. N. Sugimoto, T. Nagashima, T. Hasegawa, S. Ohara, K. Taira, and K. Kikuchi, "Bismuth-based optical fiber with nonlinear coefficient of 1360 W^{-1} km $^{-1}$," Optical Fiber Communication Conference (OFC'04), PDP26, Los Angeles, Feb. 2004.
8. Y.Takushima, F.Futami, and K. Kikuchi, "Generation of over 140-nm-wide super-continuum from a normal dispersion fiber by using a mode-locked semiconductor laser source," IEEE Photonics Technol. Lett., vol.10, no.11, pp.1560-1562, 1998.
9. P.V.Mamyshev, "All-optical data regeneration based on self-modulation effect," Proc. of 24th European Conference on Optical Communications (ECOC '98), Sept.20-24, 1998, pp475-476.
10. K. Taira and K. Kikuchi, "Picosecond pulse generation with a high extinction ratio employing an electroabsorption modulator, a fiber compressor, and a self-phase-modulation-based pulse reshaper," Electron. Lett., vol.40, no.1, pp. 15-16, Jan. 2004.
11. T. Sakamoto and K.Kikuchi, "Nonlinear optical loop mirror with an optical bias controller for achieving full-swing operation of gate switching," IEEE Photonics Technol. Lett., vol.16, no.2, 545-547, 2004.
12. J. Suzuki, K. Taira, Y. Fukuchi, Y. Ozeki, T. Tanemura, and K. Kikuchi, "All-optical time-division add-drop multiplexer using an optical fiber Kerr shutter," Electron. Lett., vol.40, no.7, pp.445-446, 2004.
13. T.Tanemura and K. Kikuchi, "Unified analysis of modulational instability induced by cross-phase modulation in optical fibers,", J. Opt. Soc. Am. B, vol.20, no.12, pp.2502-2514, 2003.
14. T.Tanemura, C.S. Goh, K.Kikuchi, and S.Y. Set, "Widely tunable wavelength conversion using fiber four-wave mixing driven by two co-modulated pump waves," IEEE Photonics Technol. Lett., vol.16, no.2, pp.551-553, 2004.
15. T.Sakamoto, K.Seo, K.Taira, N.S.Moon, and K.Kikuchi, "Polarization-insensitive all-optical time-division demultiplexing using a fiber four-wave mixer with a peak-holding optical phase-locked loop," IEEE Photonics Technol. Lett., vol.16, no.2, 563-565, 2004.